Original Article
Resveratrol alleviates sepsis-induced acute lung injury by suppressing inflammation and apoptosis of alveolar macrophage cells

Lei Yang[1], Zhen Zhang[2], Yuzhen Zhuo[1], Lihua Cui[1], Caixia Li[1], Dihua Li[1], Shukun Zhang[1], Naiqiang Cui[3], Ximo Wang[2,3], Hongwei Gao[4]

[1]Tianjin Institute of Acute Abdominal Disease of Integrated Traditional Chinese and Western Medicine, Tianjin 300100, China; [2]Graduate School of Tianjin Medical University, Tianjin 300070, China; [3]Department of Surgery, Tianjin Hospital of Integrated Traditional Chinese and Western Medicine, Tianjin 300100, China; [4]Department of Anesthesiology, Perioperative & Pain Medicine, Brigham and Women's Hospital, Harvard Medical School, Boston 02115, MA

Abstract: Sepsis is a major cause of death in intensive care units. The purpose of this study was to investigate the effect of resveratrol (RSV) on sepsis-induced acute lung injury (ALI). The underlying molecular mechanisms were deciphered by both *in vitro* and *in vivo* experiments. Polymicrobial sepsis was induced in C57BL/6 mice by cecal ligation and puncture (CLP). RSV pretreatment significantly attenuated CLP-induced acute lung injury, which was associated with enhanced expression of VEGF-B. The protective properties of RSV were assayed in lipopolysaccharide (LPS)-stimulated MH-S cells. We determine that RSV administration inhibited the increased production of TNF-α, IL-6, and IL-1β in LPS-stimulated MH-S cells, which was associated with inhibition of the nuclear factor-κB, P38, and ERK signaling pathways. We also provide evidence that RSV administration reduced LPS-induced apoptosis of MH-S cells by altering the unbalance of Bax/Bcl-2 and inhibiting LPS-induced autophagy. The inhibitory effects of RSV on cytokine levels and apoptosis of alveolar macrophages were both blocked by VEGF-B siRNA. Furthermore, RSV administration regulated LPS-induced C5aR and C5L2 expression, revealing an additional mechanism underlying RSV's anti-inflammatory and anti-apoptosis effects. Collectively, these results demonstrated that RSV was able to protect against sepsis-induced acute lung injury by activating the VEGF-B signaling pathway.

Keywords: RSV, acute lung injury, alveolar macrophages, anti-apoptosis, anti-inflammation, VEGF-B

Introduction

Despite improvements in supportive treatment for acute lung injury (ALI), ALI is common and devastating clinical disorders with high morbidity and mortality [1]. The pathophysiology of ALI is characterized by complex mechanisms that involve cell inflammation, cytokines, as well as abnormal apoptosis of pulmonary cells, including pulmonary alveolar type II epithelial cells, pulmonary vascular endothelial cells, alveolar macrophages (AMs) [2-5]. AMs account for about 90% of the cells in the bronchoalveolar lavage fluid (BALF) and play an important role in the pathogenesis of ALI [6]. Many current studies have indicated a consistent association between AMs and ALI in humans and ani-

mal models [7-9], because AMs apoptosis and dysfunction occur late in sepsis, which is implicated in the increased mortality [10]. However, little is known about the intracellular signaling pathways that regulate the fate of AMs in ALI, and efforts directed towards the accurate mechanisms to improve ALI detection and treatments are indispensable. Discovering new drugs and new strategies therefore remains an urgent therapeutic challenge in the treatment of ALI.

Resveratrol (3, 5, 4'-trans-trihydroxystilbene; RSV), a potent activator of SIRT-1 [11] present in mulberries, peanuts, and grape skins [12, 13], is known for its anti-inflammatory, anti-oxidative and anti-apoptotic properties in multiple

organs, including the lungs [14, 15]. Emerging studies have reported that RSV has protective effect in sepsis. It can significantly extend the life span of septic animals and reduce acute lung injury in a LPS-induced sepsis mouse model [16, 17]. RSV could attenuate the apoptosis of pulmonary microvascular endothelial cells (PMVECs) and suppresse ox-LDL-induced macrophage apoptosis [18, 19]. However, the molecular mechanisms underlying the protective effects of RSV in septic ALI remain poorly understood.

The VEGF family includes five major factors: VEGF-A, VEGF-B, VEGF-C, VEGF-D, and placental growth factor [20]. VEGF-B bind to VEGF-receptor 1 (VEGFR-1) and the neuropilin-1 (NRP-1) coreceptor, which are expressed in lung and lung macrophages [21, 22]. Recently, VEGF-B was found as a key regulator of endothelial fatty acid uptake and insulin sensitivity [23, 24]. Its anti-cancer and neuroprotective effects were reported [25, 26]. In addition, VEGF-B expression is reduced in human heart disease, and VEGFB mRNA expression is significantly increased in the hypoxic lung [27, 28]. However, unlike VEGF-A, VEGF-B played a potent antiapoptotic effect while lacking a general antigenic activity [29, 30]. VEGF-B treatment by intravitreal injection markedly reduced retinal apoptosis in streptozotocin (STZ)-induced diabetes rats [31]. However, the functions of VEGFB in macrophages under septic conditions remain poorly understood.

In the previous study, we have first identified the relationship between RSV treatment and the expression of VEGF-B [32]; we also found that RSV attenuates myocardial ischemia/reperfusion injury through upregulation of VEGF-B [33]. The purpose of this study was to investigate the protective mechanisms of RSV in sepsis-induced acute lung injury, particularly with regard to the VEGF-B signaling.

Materials and methods

Animals and experimental designs

SPF C57BL/6 male mice were purchased from China Laboratory Animal Resource Center of National Institute for Food and Drug Control. The experimental protocol was approved by the Medicine Ethical Committee of Tianjin Nankai Hospital. Mice were acclimatized for at least 1

week before use. Mice were fasted but had free access to water starting 12 h before the surgery. A median incision was made in the lower abdomen after anesthesia, skin was prepared and disinfected, and the cecum was slightly taken out of the incision. A 4-0 braided silk suture was passed through the midpoint between the colon root and cecum terminal, which was used to tighten the cecum while avoiding the cecum artery. After that, a 21 gauge 1 inch needle was used to penetrate the cecum ligation, from which a small drop of intestinal contents was squeezed after the needle was withdrawn, followed by cecum reposition and abdomen closure. For the sham group, the abdomen was opened, cecum exposed and repositioned, and incision closed. After successful modeling, mice in the CLP+ RSV group immediately received RSV (40 mg/ kg body weight).

Cell culture

MH-S cells were obtained from the American Type Culture Collection (Manassas, VA, USA). Cells were cultured in RPMI 1640 medium supplemented with 10 mM HEPES, 2 mM l-glutamine, 100 U/ml streptomycin, 100 U/ml penicillin, and 10% (v/v) FBS. Cells (approximately 1×10^6 cells/ml) were seeded in 6-well plates before being subjected to treatments. RSV at 50 µM was added 2 h before LPS (from Escherichia coli, Sigma) stimulation.

Histologic examination and grading

After the animals were killed, lung tissues embedded in paraffin and cut in 3 µm thick sections. Sections were stained with hematoxylin and eosin stain. The total score was calculated by adding up the individual scores of each category [34].

Pulmonary MPO activity

MPO activity, an indicator of polymorphonuclear leukocytes accumulation, was determined using an MPO kit produced by Jiancheng Bioengineering Institute (Nanjing, China) according to the manufacturer's instruction.

Cell-viability assay

The cell viability in the various treatment groups was assessed with an MTT assay. In this assay, MH-S cells were rested in 96-well plates (5,000

cells/well). Following incubation with RSV (10 μM) for 2 h, cells were subsequently treated with different concentrations of LPS in complete medium for 24 h. Subsequently, 10 μl MTT was added to each well, and the plates were incubated for an additional four hours at 37°C. Subsequently, media was carefully discarded and 100 μl of dimethyl sulfoxide were added to dissolve the formazan crystals, then the 96-well plates were put on a horizontal oscillator for ten minutes. The absorbance values were measured by the enzyme mark instrument at a wavelength of 490 and a reference wavelength of 570 nm.

Measurement of apoptosis by flow cytometry analysis using the PI/Annexin V double-staining method

Cells were harvested and washed three times with cold PBS, then stained with 5 μL Annexin V-FITC and 10 μL propidium iodide (PI) for 15 min at room temperature in 500 mL of the binding buffer. Surface exposure of phosphatidylserine in apoptotic cells was measured by an Annexin V-FITC apoptosis detection kit according to the manufacturer's instructions, and then the cells were analyzed with a FACSCalibur flow cytometer (BD Biosciences).

Immunofluorescence staining

After drug treatment, cells were blocked with 10% normal fetal bovine serum for 15 min at room temperature. Subsequently, cells were incubated with mouse anti-C5aR (Hycult biotech) antibody for 1 h at 4°C. After a washing with PBS, cells were incubated with the donkey anti-rat IgG (Abcam) for a further 30 min on ice in the dark. Cells were washed twice with PBS and analyzed using FACSCalibur (BD Biosciences). Mean fluorescence intensity (MFI) was calculated using CellQuest Pro™ software (BD Biosciences).

RNA interference

Independent siRNA sequences were used to silence VEGF-B expression. The sequences used were as follows: sense, 5'-GGUGCCAUG-GAUAGACGUUTT (dTdT)-3' and anti-sense, 5'-AACGUCUAUCCAUGGCACCTT (dTdT)-3'. MH-S cells were transfected with control siRNA or VEGF-B siRNA (Shanghai GenePharma) by using the supplied transfection reagents accord-

ing to the manufacturer's instructions. At 24 hr after transfection, the cells were incubated with RSV followed by LPS treatment.

RNA extraction and quantitative real-time polymerase chain reaction

Total RNA was isolated using trizol reagent (Takara Bio, Japan) according to the manufacturer's protocol. Reverse transcription reactions were performed using a 1 μg total RNA with TransGen Reverse Transcription Kit from Applied Biosystems. Quantitative real-time PCR detection of gene expression was performed using SYBR Green Master Mix (Promega, China) in a Bio-Rad IQ5 detection system and the cycle threshold (CT) values were automatically determined in triplicates and averaged. The following primers were used for qPCR: TNF-α, forward primer, 5'-CGTCAGCCGATTTGCTATCT-3', and reverse primer, 5'-CGGACTCCGCAA-AGTCTAAG-3'; IL-6, forward primer, 5'-AGTTGC-CTTCTTGGGGACTGA-3', and reverse primer, 5'-TCCACGATTTCCCAGAGAAC-3'; IL-1β, forward primer, 5'-CTATGTCTTGCCCGTGGAG-3', and reverse primer, 5'-CATCATCCCACGAGTCACA-3'; VEGF-B, forward primer, 5'-TTCACAGGGAGA-AGAGTGGAGC-3', and reverse primer, 5'-TCC-CGTTATTGGTAGAAGTTTGG-3'; C5aR, forward primer, 5'-ACTCCCTGTGCGTGTCCC-3', and reverse primer, 5'-CCCTGCCCACTGAATCCTC-3'; C5L2, forward primer, 5'-GGCATCTCAGACACC-ATTTCG-3', and reverse primer, 5'-TTTCATTTG-CTGGACCCCTTAT-3'; GADPH, forward primer, 5'-GCCTCGTCTCATAGACAAGATG-3', and reverse primer, 5'-CAGTAGACTCCACGACATAC-3'.

Western blot analysis

Cells were lysed and incubated for 30 min in ice-cold RIPA buffer. Equal amounts of protein were subjected to SDS-PAGE for separation. After transferring onto the PVDF membrane, blocking with 5% fat-free milk. Expressions of Bax, Bcl-2, NF-κB, P-NF-κB, ERK1/2, P-ERK1/2, p38, P-P38 (Cell Signalling), LC3 (Novus) and GAPDH (Abcam) proteins were determined using respective specific antibodies (1/1000).

Statistical analysis

All the calculations were conducted using SPSS 17.0 software), and data charts were made using Prism 5.0 (GraphPad Software). All values are expressed as mean ± SEM. Values of
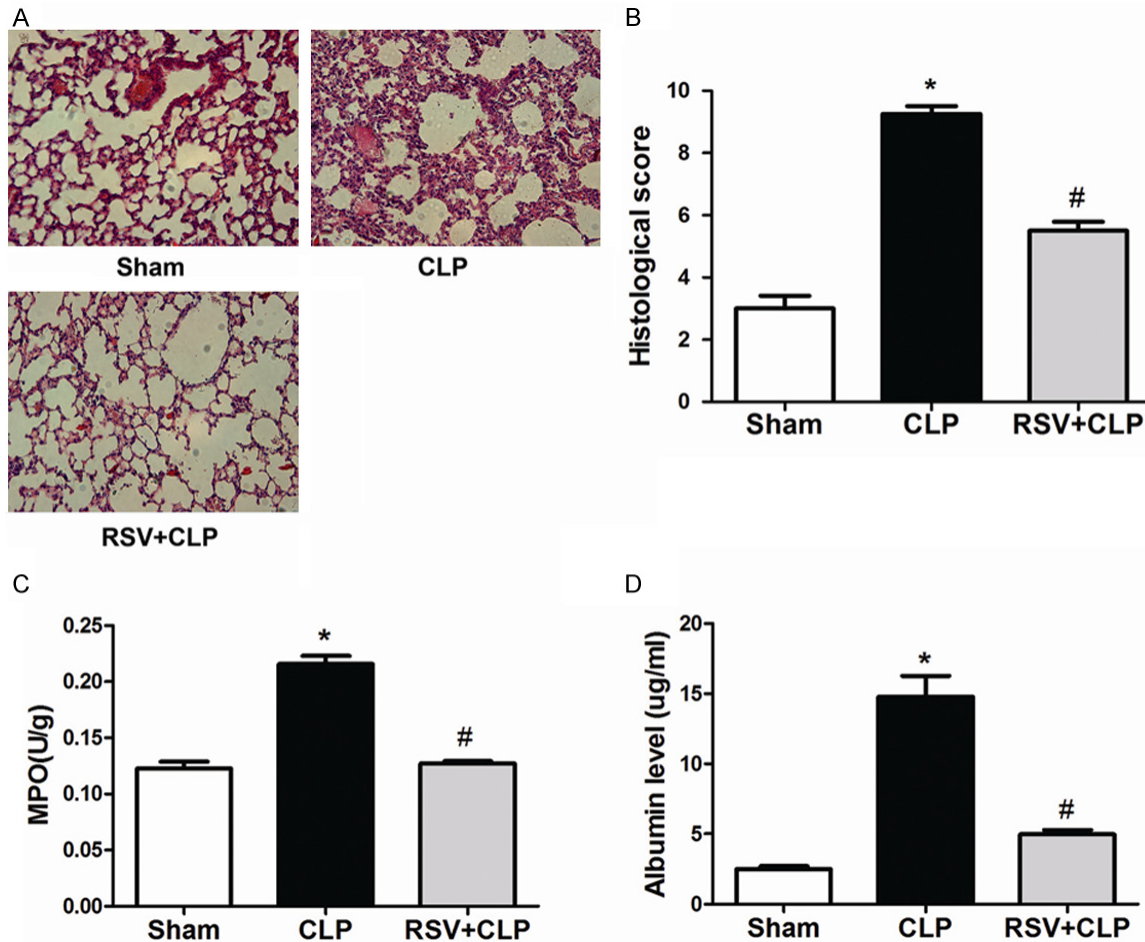
Figure 1. Treatment with RSV protected against CLP-induced acute lung injury. RSV alleviated sepsis-induced acute lung injury. A. Lung tissue sections stained with hematoxylin and eosin (original magnification 200×; scale bar 50 μm). B. Semi-quantitative analysis of lung tissues by lung injury score. C. MPO activity in lung tissues. D. Albumin level in BAL fluids was determined 24 h after CLP administration. The values presented are means ± SEM. (n = 6 in each group).*$P<0.01$ compared with the SHAM group, #$P<0.01$ compared with the CLP group.

$P<0.05$ were considered a statistically significant difference. Data sets were analyzed using one-way analysis of variance, and pairwise comparison was conducted using the Student-Newman-Keuls test.

Results

Treatment with RSV protected against CLP-induced acute lung injury

To evaluate the protective effect of RSV in CLP-induced acute lung injury, histological analyses of lung tissues were performed. As shown in **Figure 1A** and **1B**, at 24 h after sepsis, histopathology of the lung sections demonstrated an acute inflammatory response including interstitial edema and thickening with inflammatory cell infiltration, microvascular congestion, and alveolar integrity destruction. Meanwhile, histological damage was visibly alleviated in the RSV group compared with the CLP group. As shown in **Figure 1C** and **1D**, compared with the sham group, MPO activity of the lung tissues was elevated in the CLP group, (P<0.01), while RSV decreased MPO activity of lung tissues in CLP mice. In addition, the albumin level in BAL fluids was elevated in the CLP group; however, RSV significantly reduced albumin content in the BAL fluids from CLP mice (P <0.01).

Treatment with RSV suppressed production of proinflammatory cytokines by upregulating the expression of VEGF-B both in vivo and in vitro

To evaluate the protective effect of RSV on CLP-induced lung inflammatory response, pro-
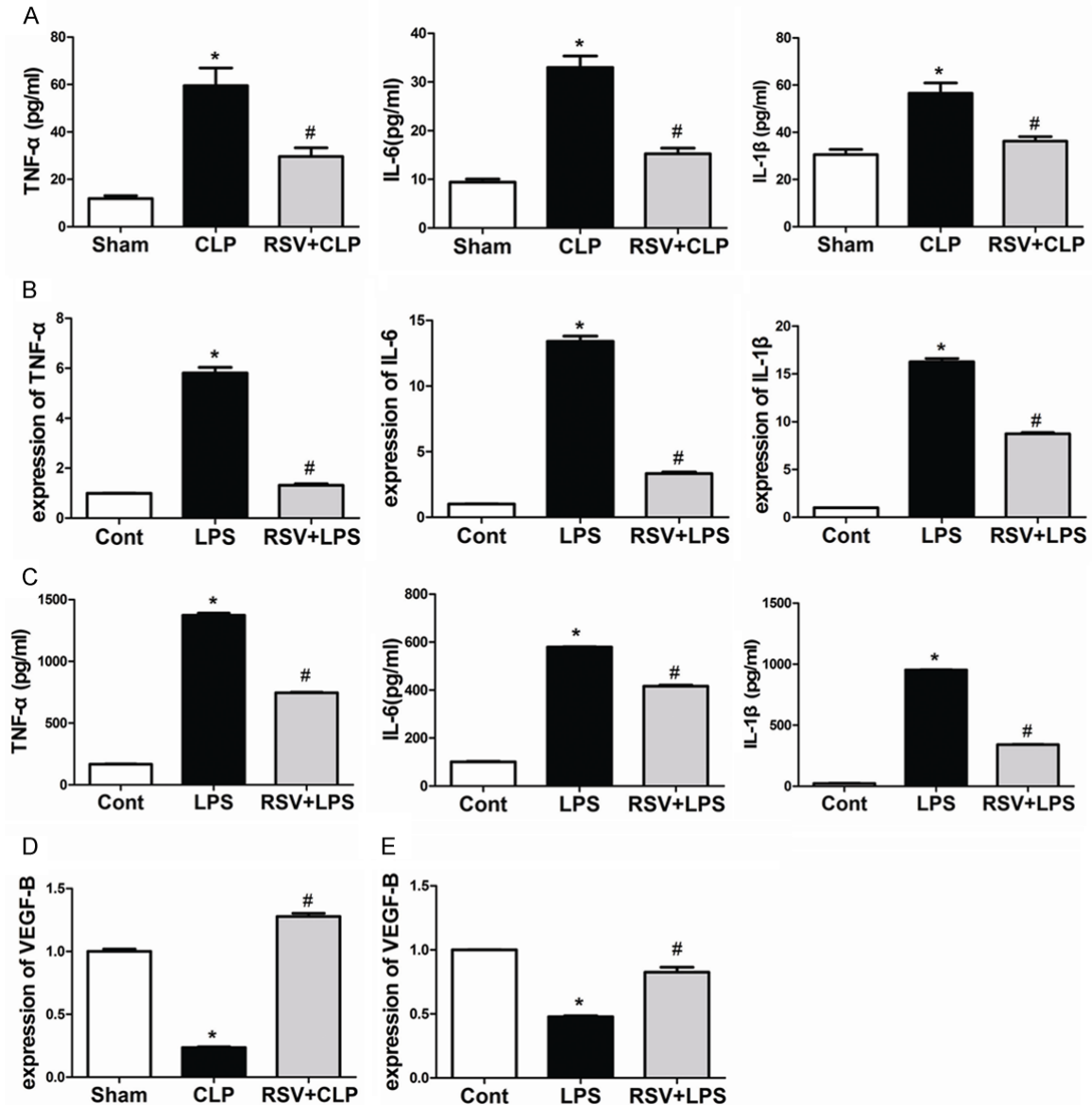
Figure 2. Treatment with RSV suppressed production of proinflammatory cytokines by upregulating the expression of VEGF-B both *in vivo* and *in vitro*. RSV inhibited the inflammatory response both in vivo and in vitro (A) Bronchoalveolar lavage fluid collected at 24 h after surgery to analyze inflammatory cytokines. *$P<0.05$ compared with the SHAM group, #$P<0.05$ compared with the CLP group. (B) The mRNA expression levels of TNF-α, IL-1β, and IL-6 (n = 4). Cells were exposed to 100 ng/mL LPS for 1 h. (C) Cell culture media were collected and the concentrations of TNF-α, IL-1β, and IL-6 were measured by ELISA (n = 4) (D) Lungs were harvested 24 h after surgery, and mRNA levels of VEGF-B were quantified by real-time PCR. (D) The mRNA expression levels of VEGF-B in Cells were quantified by real-time PCR (n = 3). *$P<0.01$ compared with the control group, #$P<0.01$ compared with the LPS group.

inflammatory cytokines were examined in BAL fluids. As shown in **Figure 2A** , compared with the sham group, levels of TNF-α, IL-1β, and IL-6 were significantly elevated in the CLP group, (P<0.01); meanwhile, this increase was significantly attenuated by RSV treatment. Macrophages are important cells involved in inflammation by secreting various inflammatory

mediators. Therefore, we sought to determine the effects of RSV treatment on the secretion of proinflammatory mediators from LPS-stimulated alveolar macrophages. As shown in **Figure 2B**, levels of TNF-α, IL-6, and IL-1β mRNA markedly increased in MH-S cells, an alveolar macrophage cell line, after 1 h of LPS exposure. Results were acquired by real-time PCR.
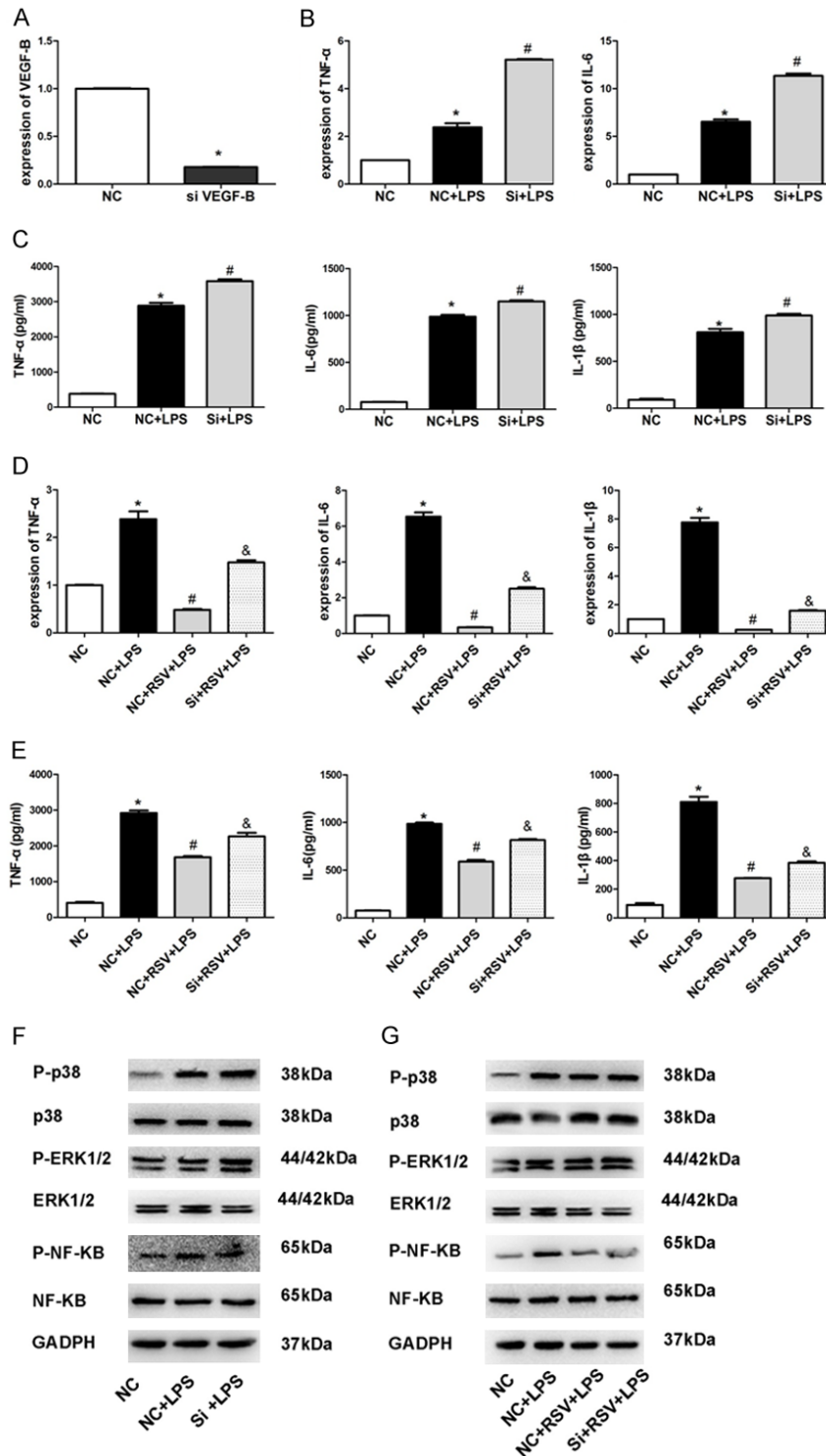
Figure 3. VEGF-B siRNA abolished inhibitory effect of RSV on inflammation. Efficiency of VEGF-B knockdown by using siRNA in MH-S cells. A. Levels of VEGF-B in MH-S cells after siRNA treatment. B. The mRNA expression levels of TNF-α, IL-6, and IL-1β. C. Concentrations of TNF-α, IL-6, and IL-1β measured by ELISA (n = 3). D. The mRNA expression levels of TNF-α, IL-6, and IL-1β (n = 3). E. Concentrations of TNF-α, IL-6, and IL-1β measured by ELISA (n = 3). F. NF-κB/P-NF-κB, ERK1/2/P-ERK1/2 and p38/P-P38 protein levels after siRNA treatment in MH-S cells. G. NF-κB/P-NF-κB, ERK1/2/P-ERK1/2, and p38/P-P38 protein levels after siRNA treatment in MH-S cells. *$P<0.01$ compared with the NC group, #$P<0.01$ compared with the NC+LPS group, &$P<0.05$ compared with the NC+RSV+LPS group.

This increase in TNF-α, IL-6, and IL-1β mRNA was significantly attenuated by RSV treatment. As shown in **Figure 2C**, cytokine secretions in MH-S cells were evaluated by enzyme-linked immunosorbent assay (ELISA), which showed that levels of TNF-α, IL-6, and IL-1β were also noticeably attenuated by RSV treatment.

VEGF-B is abundantly expressed in tissues with highly active energy metabolism, such as in the heart, lung, endothelial cells, and macrophages. As shown in **Figure 2D**, with 24 h of CLP-induced sepsis, the mRNA expression of VEGF-B was significantly decreased in the lung compared with saline-treated controls. In addi-

tion, we showed that VEGF-B expression was efficiently up-regulated by RSV treatment. After treatment with LPS, the mRNA expression of VEGF-B was significantly decreased in MH-S cells, while RSV treatment significantly increased its expression in MH-S cells (**Figure 2E**).

VEGF-B siRNA abolished inhibitory effect of RSV on inflammation

We performed further experiments to determine whether VEGF-B was responsible for RSV-mediated secretion of proinflammatory mediators in MH-S cells. As shown in **Figure 3A**, VEGF-B expression was efficiently down-regulated by siRNA specific for VEGF-B in MH-S cells. These results were determined using real-time PCR. As shown in **Figure 3B** and **3C**, the expression and secretion of TNF-α, IL-6, and IL-1β were all significantly induced from LPS-stimulated MH-S cells. Moreover, silencing VEGF-B led to a significant increase in LPS-induced secretion of TNF-α, IL-6, and IL-1β from MH-S cells when compared with control siRNA-treated cells. Importantly, knockdown of VEGF-B abolished RSV-mediated expression and secretion of proinflammatory mediators (**Figure 3D**, **3E**).

The NF-κB and mitogen-activated protein kinase (MAPK) are 2 key pathways for LPS-stimulated signaling events [26]. Hence, we tested whether the suppression of proinflammatory cytokines was regulated through these pathways. As shown in **Figure 3F**, LPS strongly activated NF-κB, ERK1/2, and p38 in MH-S cells, while RSV prevented LPS-induced increase in levels of phosphorylated NF-κB, ERK1/2, and p38. Furthermore, knockdown of VEGF-B abolished RSV-mediated inhibition of NF-κB, ERK1/2, and p38. Additional experiments showed that silencing VEGF-B led to a significant increase in LPS-induced activation of NF-κB, ERK1/2, and p38 in MH-S cells compared with control siRNA-treated cells (**Figure 3G**).

RSV promotes cell viability and protects LPS-induced apoptosis in MH-S cells

To determine the working concentration of LPS, MH-S cells were cultured in 1640 supplemented with different concentrations of LPS

(0, 100, 150, 200, 250 and 300 µg/mL) for 24 h, in which cell viability was evaluated using the MTT assay. LPS decreased the cell viability with dose increasing (**Figure 4A**). Based on this result, we used 150 µg/mL LPS in the subsequent experiments. Next, we investigated whether RSV exerted a protective effect on MH-S cells exposed to LPS. We pre-treated MH-S cells with 10 µM RSV (2 h) prior to LPS (150 µg/mL) exposure for 24 h, in which RSV augmented the decline of cell viability as a result of LPS insult (**Figure 4B**). To quantify the protective action of RSV against cytotoxic effects of LPS, we pre-treated MH-S cells with RSV (2 h) and then incubated them with LPS (150 µg/mL) for 24 h. Apoptosis was assessed by Annexin V-FITC and PI double staining. The sum of the early apoptotic cells (quadrant 4, Q4) and late apoptotic cells (quadrant 2, Q2). The apoptotic rate was defined as the number of apoptotic cells to the number of all cells. The apoptosis rate was increased significantly when cells were treated with 150 mg/mL LPS compared with the controls. However, RSV caused a significant reduction of early apoptotic cells as compared with the LPS (150 mg/mL) only groups (**Figure 4C**, **4D**). Together, these results demonstrate that RSV promotes cell viability and protects LPS-induced apoptosis in MH-S cells. Cell survival is dependent on the ratio of Bcl-2 (antiapoptotic) to Bax (proapoptotic). To further investigate the molecular mechanism of RSV protection in apoptosis of MH-S cells after exposed to LPS, the expressions of Bcl-2 and Bax proteins were determined by western blotting. The treatment of MH-S cells with LPS (150 mg/mL) for 4 h caused a significant increase in the level of Bax (**Figure 4E**), while reduced Bcl-2 expression resulting in a decrease in the Bcl-2/Bax ratio (**Figure 4F**). In contrast, RSV increased the Bcl-2/Bax ratio by decreasing Bax expression and simultaneously increasing Bcl-2.

RSV inhibits LPS-induced apoptosis in macrophages in part via VEGF-B signaling

To investigate the role of VEGF-B in RSV mediating anti-apoptotic effect, we inhibited expression of VEGF-B by using siRNA in MH-S cells. After treatment with VEGF-B siRNA, increased apoptosis cells were found in comparison with the group receiving only RSV treatment, indicating that RSV attenuated LPS-induced apopto-
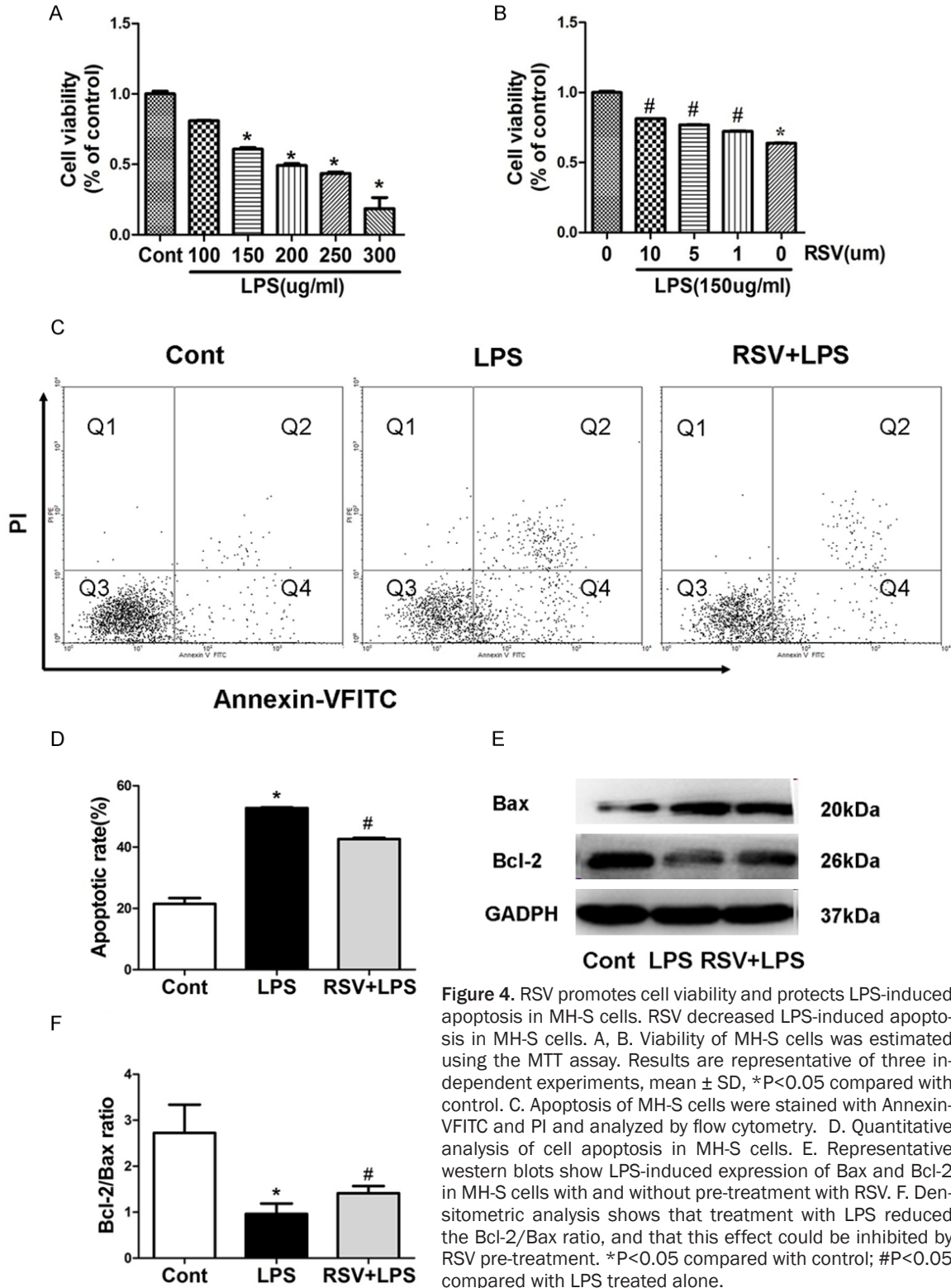
Figure 4. RSV promotes cell viability and protects LPS-induced apoptosis in MH-S cells. RSV decreased LPS-induced apoptosis in MH-S cells. A, B. Viability of MH-S cells was estimated using the MTT assay. Results are representative of three independent experiments, mean ± SD, *P<0.05 compared with control. C. Apoptosis of MH-S cells were stained with Annexin-VFITC and PI and analyzed by flow cytometry. D. Quantitative analysis of cell apoptosis in MH-S cells. E. Representative western blots show LPS-induced expression of Bax and Bcl-2 in MH-S cells with and without pre-treatment with RSV. F. Densitometric analysis shows that treatment with LPS reduced the Bcl-2/Bax ratio, and that this effect could be inhibited by RSV pre-treatment. *P<0.05 compared with control; #P<0.05 compared with LPS treated alone.

sis via the VEGF-B regulation (**Figure 5A, 5B**). Importantly, knockdown of VEGF-B blocked RSV-mediated Bcl-2 and Bax expression **Figure** 5C), suggesting that RSV regulates Bcl-2/Bax expression through the VEGF-B signaling pathway.
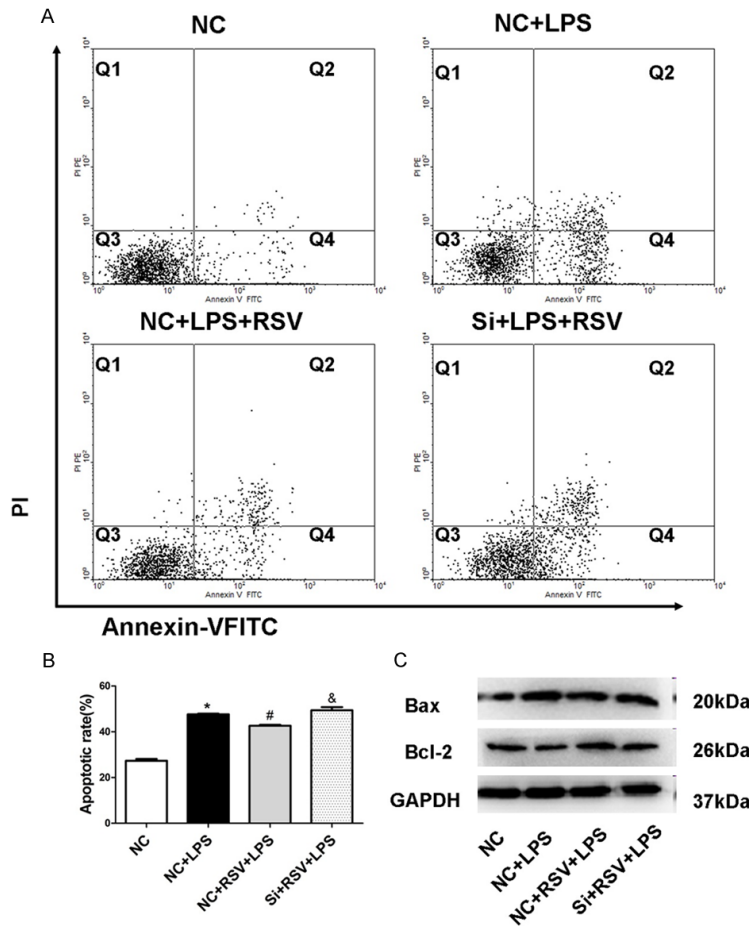
Figure 5. RSV inhibits LPS-induced apoptosis in macrophages in part via VEGF-B signaling. A. Apoptosis of MH-S cells were stained with Annexin-VFITC and PI and analyzed by flow cytometry. B. Quantitative analysis of cell apoptosis in MH-S cells. C. Bax, Bcl-2 protein levels after siRNA treatment in MH-S cells. *P<0.01 compared with the NC group, #P<0.01 compared with the NC+LPS group, &P<0.05 compared with the NC+RSV+LPS group.

pression LC3-II/I (**Figure 6C**), suggesting that RSV regulates autophagy through the VEGF-B signaling pathway.

To further explore the involvement of RSV in MH-S cell apoptosis in the LPS-induced autophagy model, the autophagy inducer rapamycin was used to determine whether RSV's effect on autophagy involved MH-S cell apoptosis. As shown in **Figure 6D** and **6E**, rapamycin reversed the RSV-mediated anti-apoptosis effects and the expression of LC3 in the LPS-induced autophagy model (**Figure 6F**), suggesting that RSV could inhibit LPS-induced cell apoptosis by blocking autophagy.

Treatment with RSV affected both mRNA and protein levels of C5aR and C5L2 in MH-S cells

The complement anaphylatoxin, C5a, is a key factor for the regulation of inflammatory responses during sepsis, and has been shown to play a critical role in survival after CLP [35]. C5a binds to receptors C5aR and C5L2, both of which are critical factors during polymicrobial sepsis after CLP [36]. We thus examined the effects of RSV on the expression of C5aR and C5L2 in MH-S cells. Real-time PCR analysis showed that the LPS-dependent induce in C5aR gene expression at 1 h was significantly decreased by RSV treatment (**Figure 7A**), and the reduction in C5L2 gene expression was significantly increased by RSV treatment (**Figure 7B**). We tested whether RSV affected the cell surface expression of C5aR and C5L2. As shown in **Figure 7C** and **7D**, LPS significantly increased C5aR expression and decreased C5L2 expression compared to the control group, while RSV treatment abrogated these effects. In summary, RSV affected both gene and protein expression of C5aR and C5L2 in MH-S cells.

RSV protects AMs against LPS-induced apoptosis in part via inhibiting LPS-induced autophagy

To determine whether RSV afected autophagy, we used monodansylcadaverine (MDC) staining to detect autophagic vacuoles. As shown in **Figure 6A**, LPS induced the accumulation of MDC-labeled vacuoles in the cytoplasm in MH-S cells, while RSV significantly lessened the accumulation of MDC-labeled vacuoles. Moreover, we determined the effect of RSV on the expression of autophagy marker LC3 by western blot. The ratio of LC3-II/I was decreased in RSV group in comparison with LPS group (**Figure 6B**). However, VEGF-B siRNA treatment markedly reversed RSV lessened expression
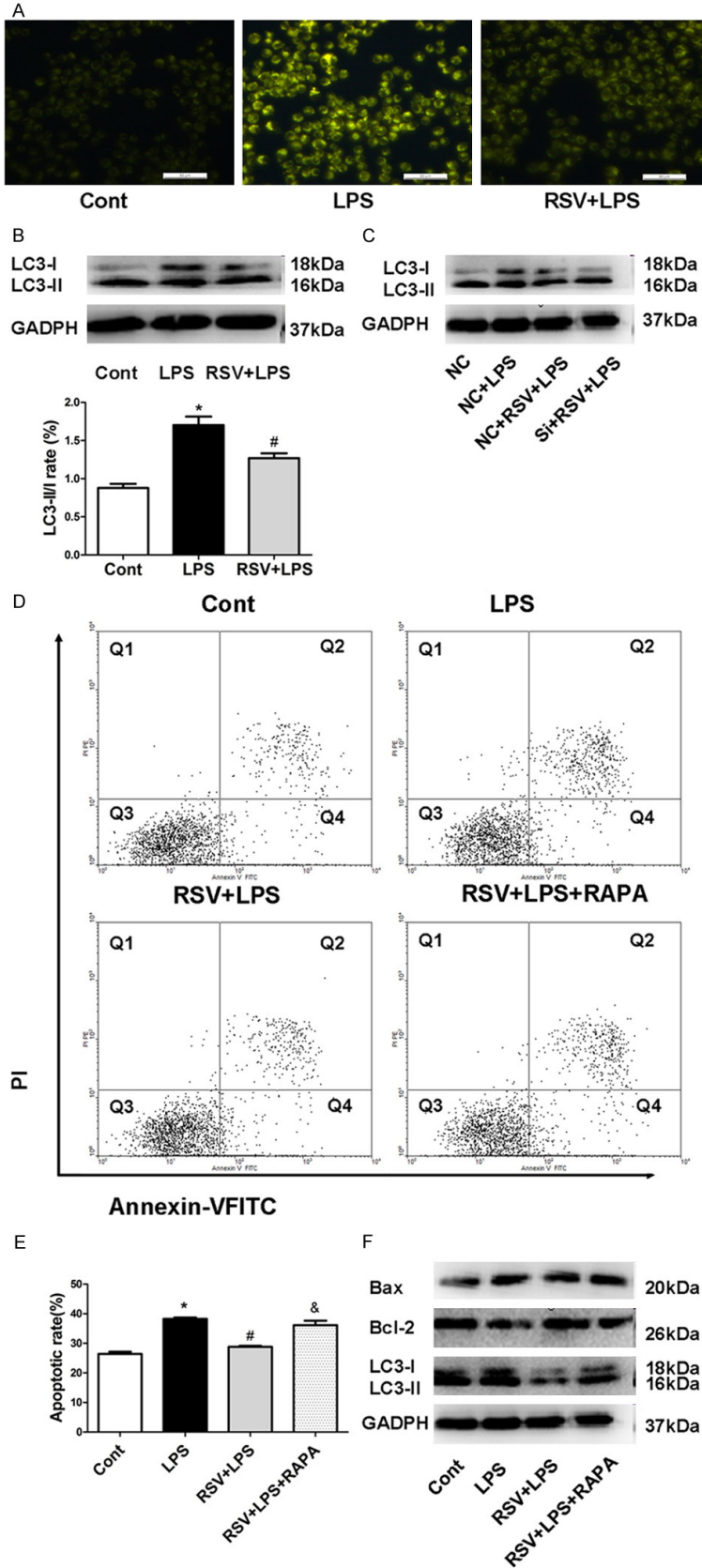
Figure 6. RSV protects AMs against LPS-induced apoptosis in part via inhibiting LPS-induced autophagy. RSV decreased LPS-induced autophagy in MH-S cells. (A) Autophagy level in MH-S cells was detected by MDC staining (B) RSV decreased protein level of LC3-II/I in MH-S cells (C) LC3-II/I protein levels after siRNA treatment in MH-S cells. (D) Cell apoptosis was detected using Annexin V/PI staining and analyzed by flow cytometry. (E) Quantitative analysis of cell apoptosis in MH-S cells. Quantitative analysis of cell apoptosis in MH-S cells, *P<0.01 compared with control. #P<0.05 compared with LPS treated alone &P<0.05 compared with the RSV+LPS group. (F) LC3-II/I expression was detected using western blot after rapamycin treatment in MH-S cells.

One mechanism by which RSV exerts effects in macrophages is via VEGF-B signaling. Therefore, we tested whether the effect of RSV on C5aR and C5L2 expression was VEGF-B-dependent. As shown in **Figure 7E** and **7F**, RSV-mediated change in C5L2 and C5aR expressions in the presence of LPS were abrogated by the knockdown of VEGF-B.

Discussion

RSV, a polyphenolic compound in red wine, was well known for its anti-inflammation and anti-apoptotic properties [37, 38]. However, its protective properties and underlying mechanisms are largely unknown in the occurrence of sepsis-induced ALI. In this study, we found that RSV pretreatment ameliorated LPS-induced ALI by inhibiting inflammation *in vivo* and *in vitro*. MPO content in mice lungs and albumin levels in BAL fluids were both significantly increased after CLP [39]. Our resulted showed MPO activity and albumin level were significantly reduced by RSV treatment. These results revealed that the effects of RSV on CLP-induced ALI are associated with a decrease of capil-
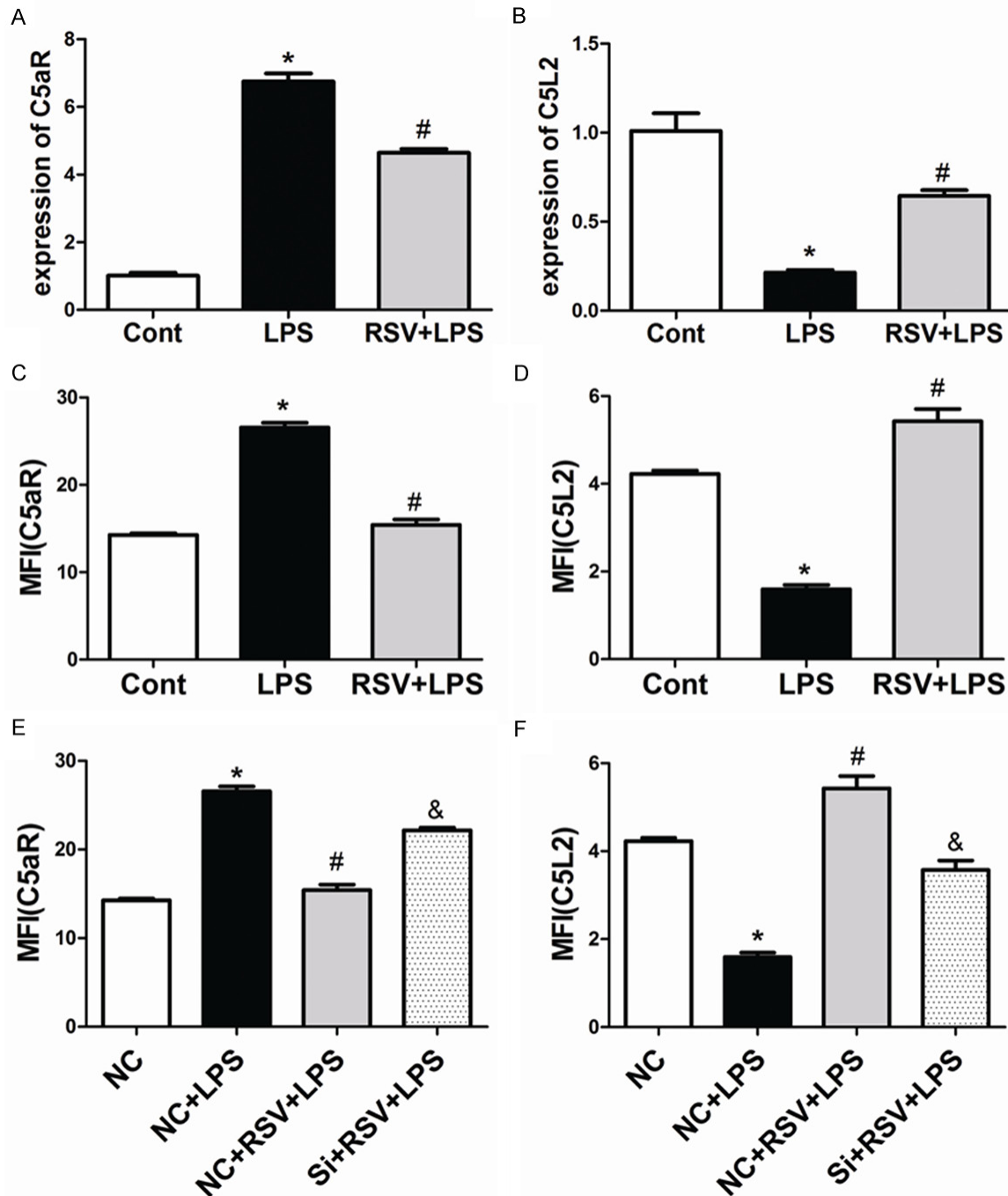
Figure 7. Treatment with RSV affected both mRNA and protein levels of C5aR and C5L2 in MH-S cells. RSV affected the expression of C5aR and C5L2 in MH-S Cells. A. The mRNA expression levels of C5aR. B. The mRNA expression levels of C5L2. C and D. Cell surface expression of C5aR and C5L2 in MH-S cells. $P<0.01$ compared with the control group, $\#P<0.01$ compared with the LPS group. E and F. Cell surface expression levels of C5aR and C5L2 after siRNA treatment in MH-S cells. $*P<0.01$ compared with the NC group, $\#P<0.01$ compared with the NC+LPS group, $\&P<0.05$ compared with the NC+RSV+LPS group.

lary permeability in lung tissues. Furthermore, we found that when RSV was given to septic mice, the elevated levels of proinflammatory cytokines in BAL fluids were greatly inhibited, and histologic damage in lungs, including in-

flammatory infiltration and parenchyma disorganization, were significantly mitigated.

In this study, we demonstrated the protective effects of RSV on CLP-induced ALI in relation to

the VEGF-B signaling pathway. VEGF can regulate inflammatory cytokine production in murine polymicrobial sepsis via regulation of C/EBPβ [40]. VEGF-C significantly attenuated proinflammatory cytokine production by regulating the PI3-kinase-Akt signaling pathway and SOCS1 expression in macrophages [41]. VEGF-B mRNA is down-regulated 6-96 h post-wounding during the acute inflammatory phase of murine excisional wounds [42]. Thus, VEGF-B might participate in the network involving acute inflammation. To further clarify the role of VEGF-B during acute inflammation. We performed *in vitro* experiments with MH-S cells. We found that silencing VEGF-B led to a significant increase in LPS-induced expression and secretion of TNF-α, IL-6, and IL-1β from MH-S cells by activation of NF-κB (P65), ERK1/2, and P38. We then tested whether VEGF-B was involved in the anti-inflammatory effects by RSV in LPS-stimulated MH-S cells. We found that VEGF-B significantly increased in the cultured macrophages upon RSV treatment. Importantly, we showed that after the knockdown of VEGF-B expression in MH-S cells, RSV was unable to attenuate LPS-induced proinflammatory cytokine production, suggesting that VEGF-B indeed plays a critical role in the anti-inflammatory effects of RSV. Previous research showed that RSV exerts anti-inflammatory effects by modulating the NF-κB and Janus kinase/STAT signaling pathways in LPS-stimulated RAW264.7 cells in a dose-dependent manner [43], and the NF-κB and MAPK pathways play central roles in the transcriptional regulation of the expression of proinflammatory genes [44]. We found that RSV inhibited activation of NF-κB (P65), ERK1/2, and P38 by enhancing the expression of VEGF-B, which was abolished by VEGF-B siRNA. This suggests that the inhibitory effect of RSV on the overproduction of proinflammatory cytokines is at least in part due to activating the VEGF-B signaling pathway.

Moreover, in our study we found that LPS reduced cell viability in dose-dependent manners by MTT assays, and a reduction in death rate of MH-S cells was observed when cells were pretreated with RSV. Furthermore, the pre-incubation of MH-S cells with RSV inhibited LPS-induced apoptosis. An increase of Bax/Bcl-2 ratio was observed at 7 days post-sepsis, illustrating the induction of apoptosis in lung tissues [45]. Our findings showed the Bax/Bcl-2 ratio was increased by LPS insult, whereas RSV treatment completely restored Bax/Bcl-2 ratio to normal levels by enhancing the expression of VEGF-B. A recent study shows that autophagy and apoptosis might play distinct roles at different stages of LPS-induced ALI. Autophagy reached a peak at 2 hr; however, apoptosis reached its maximal level at later stages (6 hr) [46]. We found that LPS can also induce autophagy in MH-S cells and RSV reversed the LPS-induced increase in LC3 levels. Li GH, Luo B, et al. reported that VEGF-B inhibited I/R-induced autophagy in rat cardiomyocytes [47]. We then tested whether VEGF-B was involved in anti- autophagy by RSV in LPS-stimulated MH-S cells. We showed in our study that knockdown of VEGF-B expression in the MH-S cells made RSV no longer able to attenuate LPS-induced increase in LC3 levels, suggesting that VEGF-B indeed plays a critical role in the anti- autophagy of RSV. VEGF-B can inhibit H9c2 cell apoptosis by inhibiting H/R-induced autophagy and autophagy may increase LPS-induced apoptosis via the intrinsic apoptotic pathway in alveolar macrophages of human silicosis [47, 48]. In the present study, we found that RSV inhibited MH-S cell apoptosis and abolished by rapamycin. Furthermore, RSV significantly up-regulated Bcl-2 and down-regulated Bax in MH-S cells by enhancing the expression of VEGF-B and was reversed by rapamycin. Therefore, the inhibitory effects of RSV on LPS-induced apoptosis in macrophages may partially via inhibiting LPS-induced autophagy.

Previous researched showed that RSV virtually completely attenuated the effects of C5a on vascular permeability, neutrophil migration, and release of proinflammatory cytokine in a C5a-induced model of acute peritonitis [49]. Acute lung injury (ALI) results in the formation of complement fragment 5a (C5a). The complement activation product, C5a interacts with its two receptors, C5aR and C5L2 [50]. C5L2 plays an important anti-inflammatory role and suppresses lipopolysaccharide-induced acute lung injury [51]. We found that RSV affected the expression of C5L2 by enhancing the expression of VEGF-B, which was abolished by VEGF-B siRNA. Our results thus indicated that suppression of LPS-induced production of proinflammatory cytokines in MH-S cells by RSV in part via regulating C5L2 expression. Furethermore, interaction of C5a with C5aR can also lead to many pathophysiological changes

as seen in acute lung injury. C5a produced during lung injury binds to C5aR can lead to apoptosis of alveolar macrophages through C5aR-mediated degradation of bcl-2 [52]. Our previous work with lung epithelial cells revealed that Silencing of C5aR reduces the severity of ALI [53]. In this study, we also found RSV inhibited the expression of C5aR by enhancing the expression of VEGF-B and was abolished by VEGF-B siRNA. Our results thus indicate that RSV protects alveolar macrophages against LPS-induced apoptosis in part via inhibiting the expression of C5aR.

In summary, we found that prophylactic treatment with RSV significantly alleviated sepsis-induced acute lung injury in mice, which was associated with anti- inflammation and anti-apoptotic effects of RSV depends on the VEGF-B signaling pathway. Therefore, RSV may be used as a potential adjuvant during sepsis-induced acute lung injury.

Conclusions

RSV could significantly improve sepsis-induced ARDS via decreasing the release of proinflammatory factors and the ratio of alveolar macrophages apoptosis. Therefore, RSV may be a promising pharmacological therapy for acute lung injury.

Acknowledgements

Disclosure of conflict of interest

None.

Address correspondence to: Dr. Ximo Wang, Graduate School of Tianjin Medical University, Tianjin 300070, China; Department of Surgery, Tianjin Hospital of Integrated Traditional Chinese and Western Medicine, Tianjin 300100, China. Tel: 86 22 2702 2268; E-mail: wangximo@126.com; Dr. Hongwei Gao, Department of Anesthesiology, Perioperative & Pain Medicine, Brigham and Women's Hospital, Harvard Medical School, Boston 02115, MA. Tel: 617-5255030; E-mail: hgao@zeus.bwh.harvard.edu

References

[1] Rubenfeld GD, Caldwell E, Peabody E, Weaver J, Martin DP, Neff M, Stern EJ and Hudson LD. Incidence and outcomes of acute lung injury. N Engl J Med 2005; 353: 1685-1693.

[2] Matthay MA, Ware LB and Zimmerman GA. The acute respiratory distress syndrome. J Clin Invest 2012; 122: 2731-2740.

[3] Huang C, Zheng H, He W, Lu G, Li X, Deng Y and Zeng M. Ghrelin ameliorates the human alveolar epithelial A549 cell apoptosis induced by lipopolysaccharide. Biochem Biophys Res Commun 2016; 474: 83-90.

[4] Gill SE, Rohan M and Mehta S. Role of pulmonary microvascular endothelial cell apoptosis in murine sepsis-induced lung injury in vivo. Respir Res 2015; 16: 109.

[5] Li B, Zeng M, He W, Huang X, Luo L, Zhang H and Deng DY. Ghrelin protects alveolar macrophages against lipopolysaccharide-induced apoptosis through growth hormone secretagogue receptor 1a-dependent c-Jun N-terminal kinase and Wnt/beta-catenin signaling and suppresses lung inflammation. Endocrinology 2015; 156: 203-217.

[6] Niesler U, Palmer A, Radermacher P and Huber-Lang MS. Role of alveolar macrophages in the inflammatory response after trauma. Shock 2014; 42: 3-10.

[7] Lu MC, Liu TA, Lee MR, Lin L and Chang WC. Apoptosis contributes to the decrement in numbers of alveolar macrophages from rats with polymicrobial sepsis. J Microbiol Immunol Infect 2002; 35: 71-77.

[8] Machado-Aranda D, V Suresh M, Yu B, Dolgachev V, Hemmila MR, Raghavendran K. Alveolar macrophage depletion increases the severity of acute inflammation following nonlethal unilateral lung contusion in mice. J Trauma Acute Care Surg 2014; 76: 982-990.

[9] Jones HD, Crother TR, Gonzalez-Villalobos RA, Jupelli M, Chen S, Dagvadorj J, Arditi M and Shimada K. The NLRP3 inflammasome is required for the development of hypoxemia in LPS/mechanical ventilation acute lung injury. Am J Respir Cell Mol Biol 2014; 50: 270-280.

[10] Pahuja M, Tran C, Wang H and Yin K. Alveolar macrophage suppression in sepsis is associated with high mobility group box 1 transmigration. Shock 2008; 29: 754-760.

[11] Arunachalam G, Yao H, Sundar IK, Caito S and Rahman I. SIRT1 regulates oxidant- and cigarette smoke-induced eNOS acetylation in endothelial cells: role of resveratrol. Biochem Biophys Res Commun 2010; 393: 66-72.

[12] Baur JA and Sinclair DA. Therapeutic potential of resveratrol: the in vivo evidence. Nat Rev Drug Discov 2006; 5: 493-506.

[13] Kumerz M, Heiss EH, Schachner D, Atanasov AG and Dirsch VM. Resveratrol inhibits migration and Rac1 activation in EGF- but not PDGF-activated vascular smooth muscle cells. Mol Nutr Food Res 2011; 55: 1230-1236.

[14] Oh YC, Kang OH, Choi JG, Chae HS, Lee YS, Brice OO, Jung HJ, Hong SH, Lee YM and Kwon DY. Anti-inflammatory effect of resveratrol by inhibition of IL-8 production in LPS-induced THP-1 cells. Am J Chin Med 2009; 37: 1203-1214.

[15] Sin TK, Yu AP, Yung BY, Yip SP, Chan LW, Wong CS, Ying M, Rudd JA and Siu PM. Modulating effect of SIRT1 activation induced by resveratrol on Foxo1-associated apoptotic signalling in senescent heart. J Physiol 2014; 592: 2535-2548.

[16] Holthoff JH, Wang Z, Seely KA, Gokden N and Mayeux PR. Resveratrol improves renal microcirculation, protects the tubular epithelium, and prolongs survival in a mouse model of sepsis-induced acute kidney injury. Kidney Int 2012; 81: 370-378.

[17] Li T, Zhang J, Feng J, Li Q, Wu L, Ye Q, Sun J, Lin Y, Zhang M, Huang R, Cheng J, Cao Y, Xiang G, Zhang J and Wu Q. Resveratrol reduces acute lung injury in a LPS induced sepsis mouse model via activation of Sirt1. Mol Med Rep 2013; 7: 1889-1895.

[18] Bai X, Fan L, He T, Jia W, Yang L, Zhang J, Liu Y, Shi J, Su L and Hu D. SIRT1 protects rat lung tissue against severe burn-induced remote ALI by attenuating the apoptosis of PMVECs via p38 MAPK signaling. Sci Rep 2015; 5: 10277.

[19] Guo R, Su Y, Liu B, Li S, Zhou S and Xu Y. Resveratrol suppresses oxidised low-density lipoprotein-induced macrophage apoptosis through inhibition of intracellular reactive oxygen species generation, LOX-1, and the p38 MAPK pathway. Cell Physiol Biochem 2014; 34: 603-616.

[20] Grimmond S, Lagercrantz J, Drinkwater C, Silins G, Townson S, Pollock P, Gotley D, Carson E, Rakar S, Nordenskjold M, Ward L, Hayward N and Weber G. Cloning and characterization of a novel human gene related to vascular endothelial growth factor. Genome Res 1996; 6: 124-131.

[21] Muhl L, Moessinger C, Adzemovic MZ, Dijkstra MH, Nilsson I, Zeitelhofer M, Hagberg CE, Huusko J, Falkevall A, Yla-Herttuala S and Eriksson U. Expression of vascular endothelial growth factor (VEGF)-B and its receptor (VEGFR1) in murine heart, lung and kidney. Cell Tissue Res 2016; 365: 51-63.

[22] Granata F, Frattini A, Loffredo S, Staiano RI, Petraroli A, Ribatti D, Oslund R, Gelb MH, Lambeau G, Marone G and Triggiani M. Production of vascular endothelial growth factors from human lung macrophages induced by group IIA and group X secreted phospholipases A2. J Immunol 2010; 184: 5232-5241.

[23] Hagberg CE, Falkevall A, Wang X, Larsson E, Huusko J, Nilsson I, van Meeteren LA, Samen E, Lu L, Vanwildemeersch M, Klar J, Genove G, Pietras K, Stone-Elander S, Claesson-Welsh L, Yla-Herttuala S, Lindahl P and Eriksson U. Vascular endothelial growth factor B controls endothelial fatty acid uptake. Nature 2010; 464: 917-921.

[24] Hagberg CE, Mehlem A, Falkevall A, Muhl L, Fam BC, Ortsater H, Scotney P, Nyqvist D, Samen E, Lu L, Stone-Elander S, Proietto J, Andrikopoulos S, Sjoholm A, Nash A and Eriksson U. Targeting VEGF-B as a novel treatment for insulin resistance and type 2 diabetes. Nature 2012; 490: 426-430.

[25] Hanrahan V, Currie MJ, Gunningham SP, Morrin HR, Scott PA, Robinson BA and Fox SB. The angiogenic switch for vascular endothelial growth factor (VEGF)-A, VEGF-B, VEGF-C, and VEGF-D in the adenoma-carcinoma sequence during colorectal cancer progression. J Pathol 2003; 200: 183-194.

[26] Guaiquil VH, Pan Z, Karagianni N, Fukuoka S, Alegre G and Rosenblatt MI. VEGF-B selectively regenerates injured peripheral neurons and restores sensory and trophic functions. Proc Natl Acad Sci U S A 2014; 111: 17272-17277.

[27] Kivela R, Bry M, Robciuc MR, Rasanen M, Taavitsainen M, Silvola JM, Saraste A, Hulmi JJ, Anisimov A, Mayranpaa MI, Lindeman JH, Eklund L, Hellberg S, Hlushchuk R, Zhuang ZW, Simons M, Djonov V, Knuuti J, Mervaala E and Alitalo K. VEGF-B-induced vascular growth leads to metabolic reprogramming and ischemia resistance in the heart. EMBO Mol Med 2014; 6: 307-321.

[28] Sands M, Howell K, Costello CM and McLoughlin P. Placenta growth factor and vascular endothelial growth factor B expression in the hypoxic lung. Respir Res 2011; 12: 17.

[29] Li Y, Zhang F, Nagai N, Tang Z, Zhang S, Scotney P, Lennartsson J, Zhu C, Qu Y, Fang C, Hua J, Matsuo O, Fong GH, Ding H, Cao Y, Becker KG, Nash A, Heldin CH and Li X. VEGF-B inhibits apoptosis via VEGFR-1-mediated suppression of the expression of BH3-only protein genes in mice and rats. J Clin Invest 2008; 118: 913-923.

[30] Bry M, Kivela R, Holopainen T, Anisimov A, Tammela T, Soronen J, Silvola J, Saraste A, Jeltsch M, Korpisalo P, Carmeliet P, Lemstrom KB, Shibuya M, Yla-Herttuala S, Alhonen L, Mervaala E, Andersson LC, Knuuti J and Alitalo K. Vascular endothelial growth factor-B acts as a coronary growth factor in transgenic rats without inducing angiogenesis, vascular leak, or inflammation. Circulation 2010; 122: 1725-1733.

[31] Huang D, Zhao C, Ju R, Kumar A, Tian G, Huang L, Zheng L, Li X, Liu L, Wang S, Ren X, Ye Z, Chen W, Xing L, Chen Q, Gao Z, Mi J, Tang Z, Wang B, Zhang S, Lee C and Li X. VEGF-B inhibits hyperglycemia- and Macugen-induced retinal apoptosis. Sci Rep 2016; 6: 26059.

[32] Yang L, Yang L, Tian W, Li J, Liu J, Zhu M, Zhang Y, Yang Y, Liu F, Zhang Q, Liu Q, Shen Y and Qi Z. Resveratrol plays dual roles in pancreatic cancer cells. J Cancer Res Clin Oncol 2014; 140: 749-755.

[33] Yang L, Zhang Y, Zhu M, Zhang Q, Wang X, Wang Y, Zhang J, Li J, Yang L, Liu J, Liu F, Yang Y, Kang L, Shen Y and Qi Z. Resveratrol attenuates myocardial ischemia/reperfusion injury through up-regulation of vascular endothelial growth factor B. Free Radic Biol Med 2016; 101: 1-9.

[34] Zhong WT, Wu YC, Xie XX, Zhou X, Wei MM, Soromou LW, Ci XX and Wang DC. Phillyrin attenuates LPS-induced pulmonary inflammation via suppression of MAPK and NF-kappaB activation in acute lung injury mice. Fitoterapia 2013; 90: 132-139.

[35] Czermak BJ, Sarma V, Pierson CL, Warner RL, Huber-Lang M, Bless NM, Schmal H, Friedl HP and Ward PA. Protective effects of C5a blockade in sepsis. Nat Med 1999; 5: 788-792.

[36] Rittirsch D, Flierl MA, Nadeau BA, Day DE, Huber-Lang M, Mackay CR, Zetoune FS, Gerard NP, Cianflone K, Kohl J, Gerard C, Sarma JV and Ward PA. Functional roles for C5a receptors in sepsis. Nat Med 2008; 14: 551-557.

[37] Trotta V, Lee WH, Loo CY, Young PM, Traini D and Scalia S. Co-spray dried resveratrol and budesonide inhalation formulation for reducing inflammation and oxidative stress in rat alveolar macrophages. Eur J Pharm Sci 2016; 86: 20-28.

[38] Liang Q, Wang XP and Chen TS. Resveratrol protects rabbit articular chondrocyte against sodium nitroprusside-induced apoptosis via scavenging ROS. Apoptosis 2014; 19: 1354-1363.

[39] Hirano Y, Aziz M, Yang WL, Wang Z, Zhou M, Ochani M, Khader A and Wang P. Neutralization of osteopontin attenuates neutrophil migration in sepsis-induced acute lung injury. Crit Care 2015; 19: 53.

[40] Nolan A, Weiden MD, Thurston G and Gold JA. Vascular endothelial growth factor blockade reduces plasma cytokines in a murine model of polymicrobial sepsis. Inflammation 2004; 28: 271-278.

[41] Zhang Y, Lu Y, Ma L, Cao X, Xiao J, Chen J, Jiao S, Gao Y, Liu C, Duan Z, Li D, He Y, Wei B and Wang H. Activation of vascular endothelial growth factor receptor-3 in macrophages restrains TLR4-NF-kappaB signaling and protects against endotoxin shock. Immunity 2014; 40: 501-514.

[42] Roy S, Khanna S, Rink C, Biswas S and Sen CK. Characterization of the acute temporal changes in excisional murine cutaneous wound inflammation by screening of the wound-edge transcriptome. Physiol Genomics 2008; 34: 162-184.

[43] Ma C, Wang Y, Dong L, Li M and Cai W. Anti-inflammatory effect of resveratrol through the suppression of NF-kappaB and JAK/STAT signaling pathways. Acta Biochim Biophys Sin (Shanghai) 2015; 47: 207-213.

[44] Campbell KJ and Perkins ND. Regulation of NF-kappaB function. Biochem Soc Symp 2006; 165-180.

[45] Chopra M, Reuben JS and Sharma AC. Acute lung injury: apoptosis and signaling mechanisms. Exp Biol Med (Maywood) 2009; 234: 361-371.

[46] Lin L, Zhang L, Yu L, Han L, Ji W, Shen H and Hu Z. Time-dependent changes of autophagy and apoptosis in lipopolysaccharide-induced rat acute lung injury. Iran J Basic Med Sci 2016; 19: 632-637.

[47] Li GH, Luo B, Lv YX, Zheng F, Wang L, Wei MX, Li XY, Zhang L, Wang JN, Chen SY, Tang JM and He X. Dual effects of VEGF-B on activating cardiomyocytes and cardiac stem cells to protect the heart against short- and long-term ischemia-reperfusion injury. J Transl Med 2016; 14: 116.

[48] Chen S, Yuan J, Yao S, Jin Y, Chen G, Tian W, Xi J, Xu Z, Weng D and Chen J. Lipopolysaccharides may aggravate apoptosis through accumulation of autophagosomes in alveolar macrophages of human silicosis. Autophagy 2015; 11: 2346-2357.

[49] Issuree PD, Pushparaj PN, Pervaiz S and Melendez AJ. Resveratrol attenuates C5a-induced inflammatory responses in vitro and in vivo by inhibiting phospholipase D and sphingosine kinase activities. FASEB J 2009; 23: 2412-2424.

[50] Sarma JV and Ward PA. New developments in C5a receptor signaling. Cell Health Cytoskelet 2012; 4: 73-82.

[51] Wang R, Lu B, Gerard C and Gerard NP. C5L2, the second C5a anaphylatoxin receptor, suppresses LPS-induced acute lung injury. Am J Respir Cell Mol Biol 2016; 55: 657-666.

[52] Sun L, Guo RF, Gao H, Sarma JV, Zetoune FS and Ward PA. Attenuation of IgG immune complex-induced acute lung injury by silencing C5aR in lung epithelial cells. FASEB J 2009; 23: 3808-3818.

[53] Hu R, Chen ZF, Yan J, Li QF, Huang Y, Xu H, Zhang X and Jiang H. Complement C5a exacerbates acute lung injury induced through autophagy-mediated alveolar macrophage apoptosis. Cell Death Dis 2014; 5: e1330.